

D-4F reduces EO6 immunoreactivity, SREBP-1c mRNA levels, and renal inflammation in LDL receptor-null mice fed a Western diet

Georgette M. Buga,^{1,*} Joy S. Frank,^{*} Giuliano A. Mottino,^{*} Ashkan Hakhamian,^{*} Ajay Narasimha,[†] Andrew D. Watson,^{*} Babak Yekta,^{*} Mohamad Navab,^{*} Srinivasa T. Reddy,^{*,†} G. M. Anantharamaiah,[§] and Alan M. Fogelman^{*}

Departments of Medicine^{*} and Molecular and Medical Pharmacology,[†] David Geffen School of Medicine at the University of California–Los Angeles, Los Angeles, CA 90095-1679; The Atherosclerosis Research Unit,[§] Department of Medicine, University of Alabama at Birmingham, Birmingham, AL 35294

Abstract LDL receptor-null (LDLR^{-/-}) mice on a Western diet (WD) develop endothelial dysfunction and atherosclerosis, which are improved by the apolipoprotein A-I (apoA-I) mimetic peptide D-4F. Focusing on the kidney, LDLR^{-/-} mice were fed a WD with D-4F or the inactive control peptide scrambled D-4F (ScD-4F) added to their drinking water. The control mice (ScD-4F) developed glomerular changes, increased immunostaining for MCP-1/CCL2 chemokine, increased macrophage CD68 and F4/80 antigens, and increased oxidized phospholipids recognized by the EO6 monoclonal antibody in both glomerular and tubulointerstitial areas. All of these parameters were significantly reduced by D-4F treatment, approaching levels found in wild-type C57BL/6J or LDLR^{-/-} mice fed a chow diet. Sterol-regulatory element binding protein-1c (SREBP-1c) mRNA levels and triglyceride levels were elevated in the kidneys of the control mice (ScD-4F) fed the WD compared with C57BL/6J and LDLR^{-/-} mice on chow ($P < 0.001$ and $P < 0.001$, respectively) and compared with D-4F-treated mice on the WD ($P < 0.01$). There was no significant difference in plasma lipids, lipoproteins, glucose, blood pressure, or renal apoB levels between D-4F- and ScD-4F-treated mice. We conclude that D-4F reduced renal oxidized phospholipids, resulting in lower expression of SREBP-1c, which, in turn, resulted in lower triglyceride content and reduced renal inflammation.—Buga, G. M., J. S. Frank, G. A. Mottino, A. Hakhamian, A. Narasimha, A. D. Watson, B. Yekta, M. Navab, S. T. Reddy, G. M. Anantharamaiah, and A. M. Fogelman. D-4F reduces EO6 immunoreactivity, SREBP-1c mRNA levels, and renal inflammation in LDL receptor-null mice fed a Western diet. *J. Lipid Res.* 2008. 49: 192–205.

Supplementary key words atherosclerosis • apolipoprotein A-I mimetic peptides • HDL • hyperlipidemia • kidney • lipoproteins • sterol-regulatory element binding protein-1

Feeding a Western diet (WD) to LDL receptor-null (LDLR^{-/-}) mice has been shown to induce atherosclerosis, endothelial dysfunction, and inflammation of brain arterioles associated with cognitive dysfunction, all of which have been reported to be significantly ameliorated by treatment with the oral apolipoprotein A-I (apoA-I) mimetic peptide D-4F without a change in plasma lipid levels or blood pressure (1–3).

In addition to hyperlipidemia, feeding a WD to LDLR^{-/-} mice results in insulin resistance and elevated plasma glucose levels (4, 5). A major problem facing Western societies is an increase in chronic renal disease that appears to be associated with dyslipidemia and diabetes in addition to hypertension (6). Dyslipidemia has been emphasized as a factor that can exacerbate hypertension-induced renal damage as well as a factor that by itself may have adverse effects on the kidney (6). Diet-induced obesity in C57BL/6J mice has been reported to cause lipid accumulation in kidneys and glomerulosclerosis via a sterol-regulatory element binding protein 1c (SREBP-1c)-dependent pathway (7).

Oxidized phospholipids have been identified as potent mediators of inflammation (8, 9). Berliner and colleagues have reported that oxidized phospholipids induce cytokine production in endothelial cells through induction of SREBP (10) via an endothelial nitric oxide synthase (eNOS)-mediated mechanism (11).

Pritchard and colleagues reported that the apoA-I mimetic peptide L-4F (identical to D-4F except that the peptide is synthesized from L-amino acids) restored the balance between nitric oxide and superoxide anion production by eNOS in LDL-treated endothelial cells in culture (12). Injection of L-4F in LDLR^{-/-} mice on a WD

Abbreviations: eNOS, endothelial nitric oxide synthase; LDLR^{-/-}, LDL receptor-null; PAS, periodic acid-Schiff; ScD-4F, scrambled D-4F; SREBP-1c, sterol-regulatory element binding protein-1c; WD, Western diet.

[†]To whom correspondence should be addressed.

e-mail: gbuga@mednet.ucla.edu

Manuscript received 9 April 2007 and in revised form 28 September 2007.

Published, JLR Papers in Press, October 9, 2007.

DOI 10.1194/jlr.M700433-JLR200

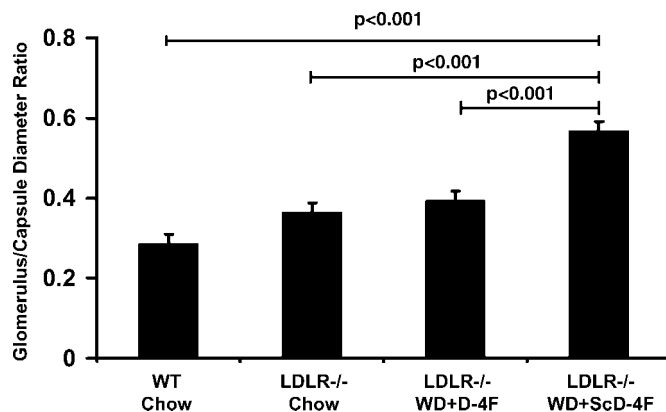


Fig. 1. The Western diet (WD) induced an increase in the glomerulus-to-capsule diameter ratio in the kidneys of LDL receptor-null (LDLR^{-/-}) mice treated with the inactive control peptide scrambled D-4F (ScD-4F) but not in mice treated with the active peptide D-4F. In the D-4F kidneys, the glomerulus-to-capsule ratio was similar to that observed in the wild-type (WT) C57BL/6J and LDLR^{-/-} mice fed a regular chow diet. Morphometry and staining were performed as described in Materials and Methods. The data shown are mean ± SEM (n = 15 mice per group).

dramatically improved eNOS-mediated vasodilation of small facial arteries (13). Pritchard and colleagues also demonstrated that oral D-4F similarly improved eNOS-mediated vasodilation in this mouse model and reduced the thickness of small artery walls if apoA-I was present (2). Tight-

skin mice have many of the myocardial and vascular features seen in scleroderma patients. Pritchard and colleagues reported that these mice also had impaired eNOS-mediated vasodilation that was significantly improved by treatment with D-4F. The tight-skin mice had elevated levels of triglycerides, which were normalized with D-4F treatment. The hearts from the tight-skin mice contained significantly higher levels of autoantibodies against oxidized phospholipids, which were reduced by D-4F treatment (14).

We previously reported that the apoA-I mimetic peptide D-4F reduced the levels of oxidized phospholipids (but not nonoxidized phospholipids) following viral infection of type II pneumocytes in vitro. This reduction in oxidized phospholipids was associated with a dramatic reduction in inflammatory parameters (15).

Given the widespread vascular inflammation reported in LDLR^{-/-} mice on a WD (1–3), we hypothesized that feeding a WD to LDLR^{-/-} mice would induce the formation of oxidized phospholipids in the kidney and would result in renal inflammation. We also hypothesized that D-4F treatment would reduce oxidized phospholipids in the kidney, which, in turn, would result in decreased renal inflammation. On the basis of the work of Jiang and colleagues (7) and Berliner and colleagues (10, 11), we also hypothesized that the WD would induce increased SREBP-1c mRNA levels and increased kidney triglyceride levels that would be ameliorated by D-4F treatment.

As shown here, feeding a WD to female LDLR^{-/-} mice for only 7 weeks induced hyperlipidemia and elevated

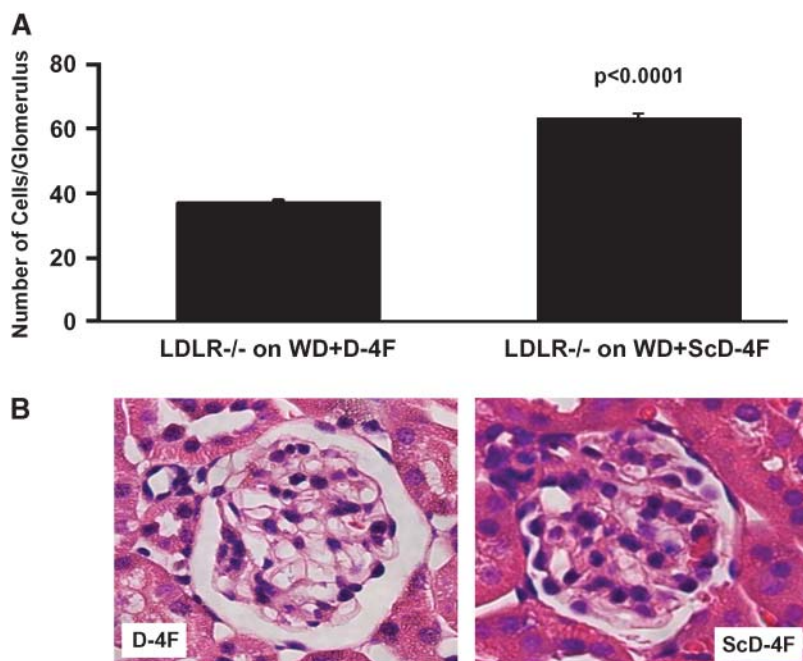


Fig. 2. A: Hypercellularity, was present in the glomeruli of LDLR^{-/-} mice on a WD treated with the inactive control peptide ScD-4F but not in the mice treated with the active peptide D-4F. The data shown are mean ± SEM (n = 10 mice per group). B: Representative examples of perfused, paraffin-embedded, and periodic acid-Schiff (PAS) reagent-stained glomeruli from D-4F (left panel) and ScD-4F mice (right panel). Note the increased number of nuclei in the glomerular tuft in the ScD-4F glomerulus. The glomerulus shown for the D-4F mice is histologically similar to the control wild-type C57BL/6J glomeruli (not shown). Magnification ×400.

plasma glucose levels, which were associated with increased kidney SREBP-1c mRNA levels, increased kidney triglyceride levels, increased kidney oxidized phospholipid levels, and renal inflammation. Treatment with oral D-4F significantly reduced the formation of oxidized phospholipids in mice fed the WD and largely prevented the increase in SREBP-1c mRNA expression elicited by the WD, prevented triglyceride accumulation in the kidneys, and significantly reduced renal inflammation without altering plasma lipids, lipoproteins, glucose, or blood pressure.

MATERIALS AND METHODS

Materials

D-4F and scrambled D-4F (ScD-4F; a control peptide with the same D-amino acids but arranged in a sequence that does not promote lipid binding, thus rendering the peptide inactive) were synthesized as described (1, 3). All other reagents were from sources previously reported (1, 3).

Mice

Female 7-week-old wild-type C57BL/6J and LDLR^{-/-} mice on a C57BL/6J background (Jackson Laboratories, Bar Harbor, ME) were maintained on a chow diet (Ralston Purina; 15% kcal from fat). Some of the LDLR^{-/-} mice were fed a WD (Teklad/Harlan, Madison, WI; diet No. 88137, 42% kcal from fat, 0.15% cholesterol, w/w) for 7 weeks. The mice receiving the WD were given either D-4F or ScD-4F at 300 μ g/ml in their drinking water. The mice consumed approximately 2.5 ml of

water per day per mouse, and there was no significant difference in water or food consumption between groups. The kidneys from some of the mice used in our studies of mouse brains (3) were collected as described below and are included in this report. The University of California, Los Angeles Animal Research Committee approved all studies.

Histology and immunohistochemistry

Mice were perfusion-fixed in 4% paraformaldehyde in PBS at pH 7.4 at physiologic pressures (75–85 mmHg for the anesthetized mice) as previously described (3). The kidneys were removed and fixed for an additional 24 h in 4% paraformaldehyde in PBS, embedded in paraffin, cut into 5 μ m sections, and stained for histological examination with hematoxylin-eosin or periodic acid-Schiff (PAS) and for immunohistochemical determination of MCP-1/CCL2 chemokine (3). Paraffin-embedded kidney sections were also used for the murine-specific monoclonal antibody EO6 against oxidized phospholipids, (16–18) and LF3 against apoB-100, respectively (19, 20). LF3 was purified from ascites using the HiTrap Protein G column (GE Healthcare Bio-Sciences AB, Uppsala, Sweden) and dialyzed in PBS using Slide-A-Lyzer Dialysis Cassettes (10K MWCO; Pierce, Rockford, IL). For identification of CD68- and F4/80-immunopositive macrophages, kidneys were embedded in OCT (Tissue-Tek; Miles Laboratories, Ltd., Elkhart, IN), rapidly frozen in isopentane at -40°C , and sectioned in a cryostat at -20°C into 8 μ m sections. The following primary antibodies and dilutions were used: F4/80 rat anti-mouse monoclonal antibody (1:100; Serotec, Raleigh, NC); CD68 rat anti-mouse monoclonal antibody (1:100; Serotec); MCP-1/CCL2 goat polyclonal antibody (1:50; Santa Cruz Biotechnology); EO6 monoclonal mouse IgM (1:2,000) was a generous gift from Dr. Joseph L. Witztum, University of Cali-

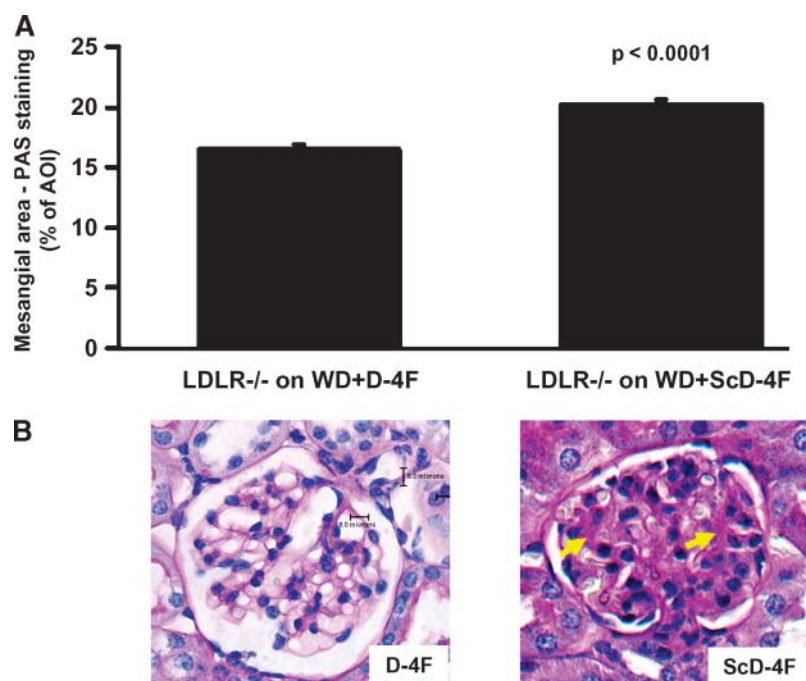


Fig. 3. A: Increased glomerular mesangial area expressed as percent of area of interest (AOI) in the kidneys of LDLR^{-/-} mice on a WD plus the inactive control peptide ScD-4F compared with LDLR^{-/-} mice on the WD plus the active peptide D-4F. The data shown are mean \pm SEM ($n = 10$ mice per group). B: Representative examples of perfused, paraffin-embedded, PAS reagent-stained glomeruli show expansion of mesangium with accumulation of PAS-positive material in the ScD-4F- (right panel) but not in the D-4F- (left panel) treated LDLR^{-/-} mice on a WD. Yellow arrows indicate PAS-positive areas of the mesangium of ScD-4F mice. Magnification $\times 400$.

fornia, San Diego; LF3 monoclonal mouse IgG (1:200) was kindly provided by Dr. S. G. Young, University of California, Los Angeles. A mouse-on-mouse basic kit was used for the murine EO6- and apoB-100 (LF3)-specific monoclonal antibodies (Vector Laboratories, Burlingame, CA). The following secondary antibodies and dilutions were used: goat anti-rat (1:200; Jackson Immuno Research Labs); donkey anti-goat (1:500; Santa Cruz Biotechnology); and biotinylated goat anti-mouse (1:200; Jackson Immuno Research Labs). Macrophage staining for F4/80, and CD68 antigens was performed on serial sections less than 8 μm apart to determine whether the antibodies localized to the same glomerulus. All immunohistochemistry sections were counterstained with hematoxylin. Negative controls for the immunostaining consisted of secondary-only antibodies in addition to isotype-matched irrelevant rat IgGs and IgM (Sigma-Aldrich, Dallas, TX).

Morphometry and associated statistical methods

All glomerular measurements were performed on 20–30 randomly selected cross sectioned glomeruli per mouse. Using an Olympus BH-2 microscope (40 \times objective), the glomeruli were photographed by means of SPOT Image software. All measurements were performed on a single focal plane. Photography, cell counting, quantitative measurements, and determination of semiquantitative parameters were performed on blinded slides. The following histological parameters were used to determine the glomerular changes (7, 21–24): *a*) glomerular tuft/Bowman's capsule diameter ratio (three measurements of the glomerular tuft and of glomerulus plus Bowman's capsule diameters were

taken for each and averaged, and the ratios were calculated); *b*) hypercellularity (determined by counting the number of nuclei in the glomerular tuft); *c*) integrity of Bowman's capsule visceral layer was determined; the coefficient of variation for three observers was $13.5 \pm 1\%$; *d*) morphology of glomerular capillaries was assessed semiquantitatively (0 = normal, + = dilated); the coefficient of variation for three observers was $9.5 \pm 1\%$; and *e*) PAS staining for mesangial area. Glomerular immunostaining for MCP-1 and for periglomerular F4/80 accumulation was quantified on 20–30 photographed glomerular cross sections per mouse after importing the images into Image Pro Plus software (Media Cybernetics, Silver Spring, MD). The number of glomeruli immunolabeled for CD68, EO6, and LF3 were counted in 20–30 high-power fields in each mouse and calculated as percent immunopositive glomeruli. Tubulo-interstitial immunostaining for MCP-1, EO6, and LF3 was quantified using Image Pro Plus software on 20–30 photographed high-power fields per mouse. For calculating the percent area of the tubulo-interstitium, three random areas of similar size (100 \times 100 μm squares) devoid of glomeruli were measured and averaged from each high-power (400 \times) microscope field. Twenty fields from each mouse were counted. The formula used for determining the percent area stained in tubulo-interstitial areas was: (labeled area/total area selected) \times 100. Statistical calculations for morphometry were performed using InStat software (Graph Pad, San Diego, CA).

Quantitative RT-PCR analysis

Total RNA was isolated from kidneys using the RNeasy Kit (Qiagen) according to the manufacturer's protocol. First-strand

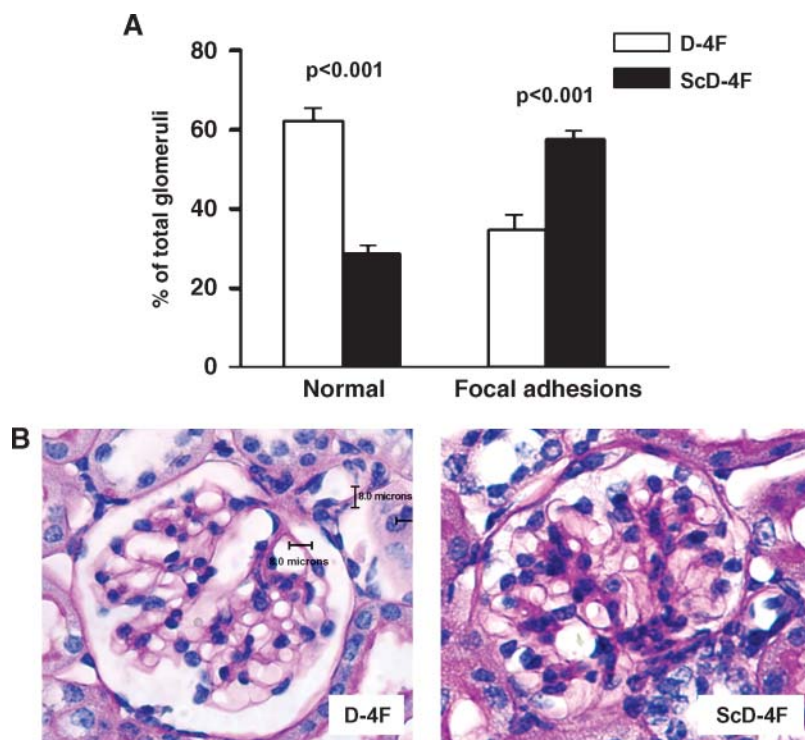


Fig. 4. A: The WD induced a decrease in the percent of normal glomeruli and an increase in the percent of glomeruli containing focal adhesions in the $\text{LDLR}^{-/-}$ mice treated with the inactive control peptide ScD-4F compared with mice treated with the active peptide D-4F. The data shown are mean \pm SEM ($n = 10$ mice per group). B: Representative examples of perfused, paraffin-embedded, PAS-stained kidney glomeruli of D-4F- (left panel) and ScD-4F- (right panel) treated $\text{LDLR}^{-/-}$ mice on a WD. Note the loss of capsular space and the presence of focal adhesions between the parietal and visceral walls of the capsule in the glomeruli of ScD-4F mice. Magnification $\times 400$.

cDNA was synthesized using random primers and Multiscribe RT (Applied Biosystems). Real-time RT-PCR was then performed on 2 μ l cDNA using iQ SYBR Green Supermix (Bio-Rad) on the MyiQ Single-color Real-time Detection System (Bio-Rad). The primers used for specific cDNA synthesis were mouse GAPDH: 5'-AAC TTT GGC ATT GTG GAA GG-3' and 5'-GGA TGC AGG GAT GAT GTT CT-3' and mouse SREBP-1c: 5'-GGA GCC ATG GAT TGC ACA TT-3' and 5'-GGC CCG GGA AGT CAC TGT-3' (25). The PCR conditions were: 95°C 3 min; 40 cycles of 95°C 30 s, 60°C 50 s, and 72°C 30 s. Values were normalized to GAPDH and calculated using the comparative C_T method.

Other procedures

Plasma blood urea nitrogen levels were determined using a colorimetric assay (Bioquart, San Diego, CA). Plasma glucose levels were measured using the ACE® clinical chemistry system (Alfa Wassermann, Inc., West Caldwell, NJ). Plasma lipoprotein and lipid levels were determined as described previously (26). Urine was spot collected and microalbuminuria determined using the competitive binding ELISA assay Albuwell M (Exocell, Philadelphia, PA). Blood pressure was determined as described previously (3).

RESULTS

D-4F prevents WD-induced histological changes in the glomerulus

Measurement of the glomerular tuft-to-Bowman's capsule diameter ratio showed a significant ($P < 0.001$) increase in the WD-fed mice treated with the control inactive

peptide ScD-4F compared with the wild-type C57BL/6J or the LDLR^{-/-} mice on chow. Addition of the active peptide D-4F to the drinking water prevented the increase in the glomerular tuft/capsule ratio observed in the ScD-4F mice. The D-4F-treated mice had values similar to those of the chow-fed LDLR^{-/-} mice (Fig. 1). To determine whether hypercellularity caused the differences in the glomerulus-to-capsule ratio, we counted the number of nuclei in the glomerulus and found a significant increase ($P < 0.0001$) in the number of cells per glomerulus in the mice on the WD receiving ScD-4F compared with those receiving D-4F (Fig. 2).

Mesangial cells proliferate in response to atherogenic lipoproteins (27–29). Using the PAS-hematoxylin stain, we determined that a significantly larger area ($P < 0.0001$) of the glomerulus was occupied by mesangial cells in the ScD-4F mice as compared with the D-4F-treated mice (Fig. 3), suggesting that the hypercellularity shown in Fig. 2 is at least in part due to an increased number of mesangial cells.

Another glomerular change that is often seen in animal models of glomerular disease is the integrity of the visceral layer of Bowman's capsule. A significantly lower percent of the ScD-4F glomeruli had a normal, clear capsular space ($P < 0.001$), and conversely, a higher percent of ScD-4F glomeruli showed focal adhesions and a disrupted visceral layer accompanied by spilling of glomerular cell content into the capsular space than was the case in the kidneys of the D-4F group (Fig. 4).

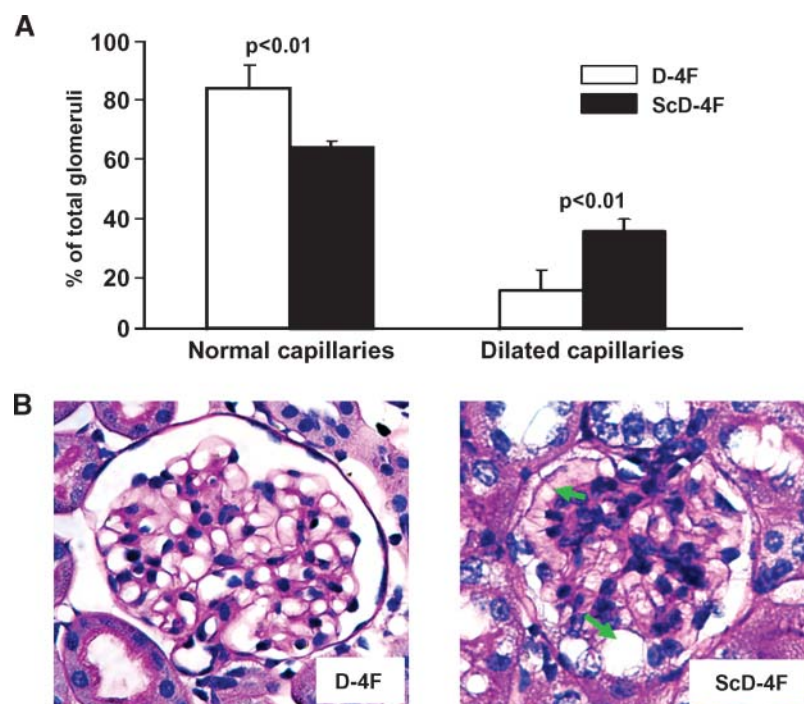


Fig. 5. A: The WD induced a decrease in the percent of glomeruli with normal, clear capillaries and an increase in the percent of glomeruli with dilated, abnormal capillaries in the kidneys of the LDLR^{-/-} mice treated with the inactive control peptide ScD-4F compared with mice treated with the active peptide D-4F. The data shown are mean \pm SEM ($n = 10$ mice per group). B: Representative examples of perfused, paraffin-embedded, PAS-stained kidney glomeruli of D-4F- (left panel) and ScD-4F- (right panel) treated LDLR^{-/-} mice on a WD. Green arrows indicate dilated capillaries in the right panel. Magnification $\times 400$.

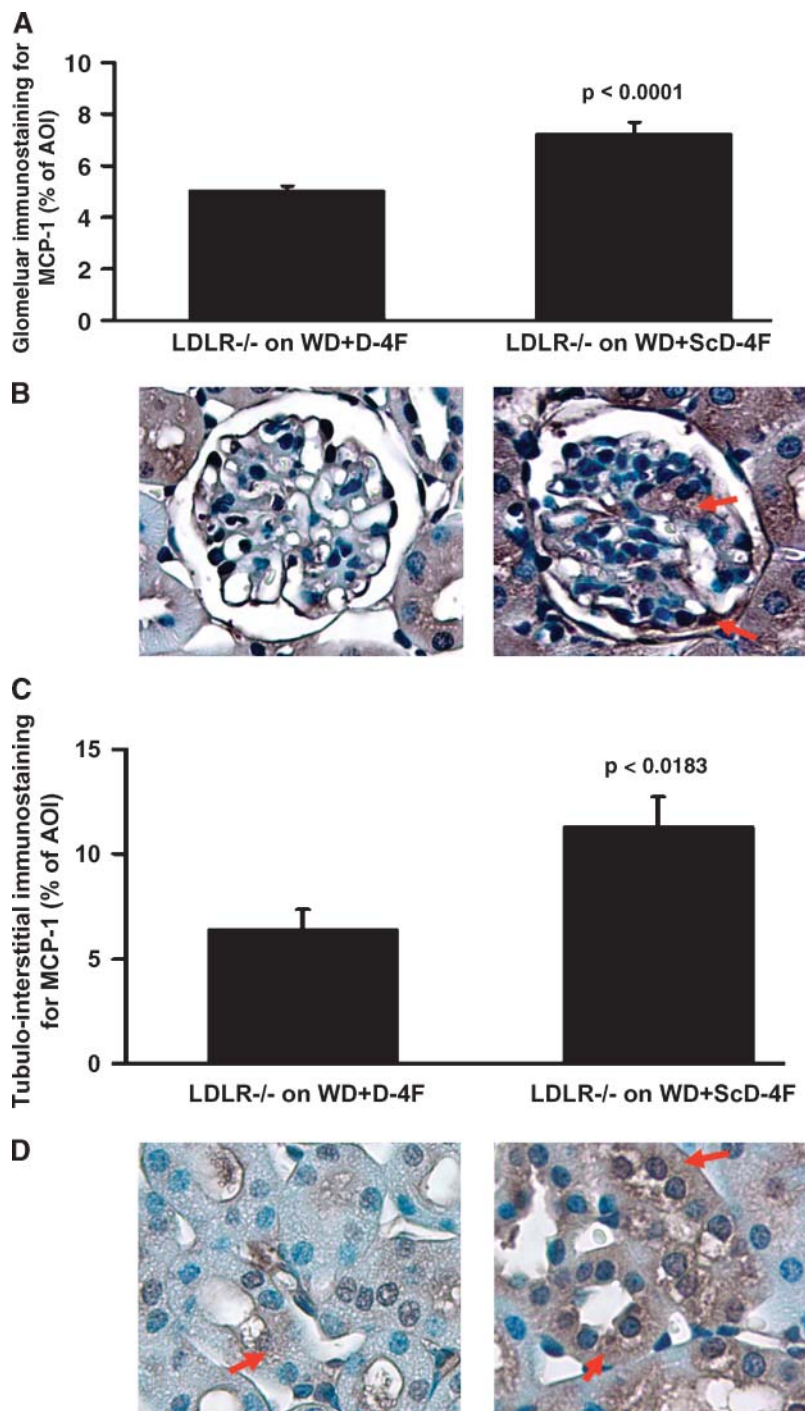


Fig. 6. A: The WD induced an increase in the percent of the glomerular tuft area (expressed as percent AOI) immunostained for monocyte chemoattractant protein-1 (MCP-1) in the kidneys of LDLR^{-/-} mice treated with the inactive control peptide ScD-4F compared with mice treated with the active peptide D-4F. B: Representative examples of paraffin-embedded sections immunostained for MCP-1 in glomeruli of D-4F- (left panel) and ScD-4F- (right panel) treated LDLR^{-/-} mice on a WD. Red arrows indicate immunostained areas in the glomerular tuft and in the capsular space in an example of local disruption of the visceral membrane of Bowman's capsule in which some of the glomerular content spilled into the capsular space. Magnification $\times 400$. C: The WD induced an increase in the percent of the tubulo-interstitial area (expressed as percent AOI) immunostained for MCP-1 in the kidneys of LDLR^{-/-} mice treated with ScD-4F compared with those of mice treated with D-4F. D: Representative examples of MCP-1-immunostained kidney cortical tubulo-interstitium of D-4F- (left panel) and ScD-4F- (right panel) treated LDLR^{-/-} mice on a WD. Red arrows indicate immunostained epithelial cells in the tubules. Final magnification $\times 400$. The data shown in A and C are mean \pm SEM (n = 10 mice per group).

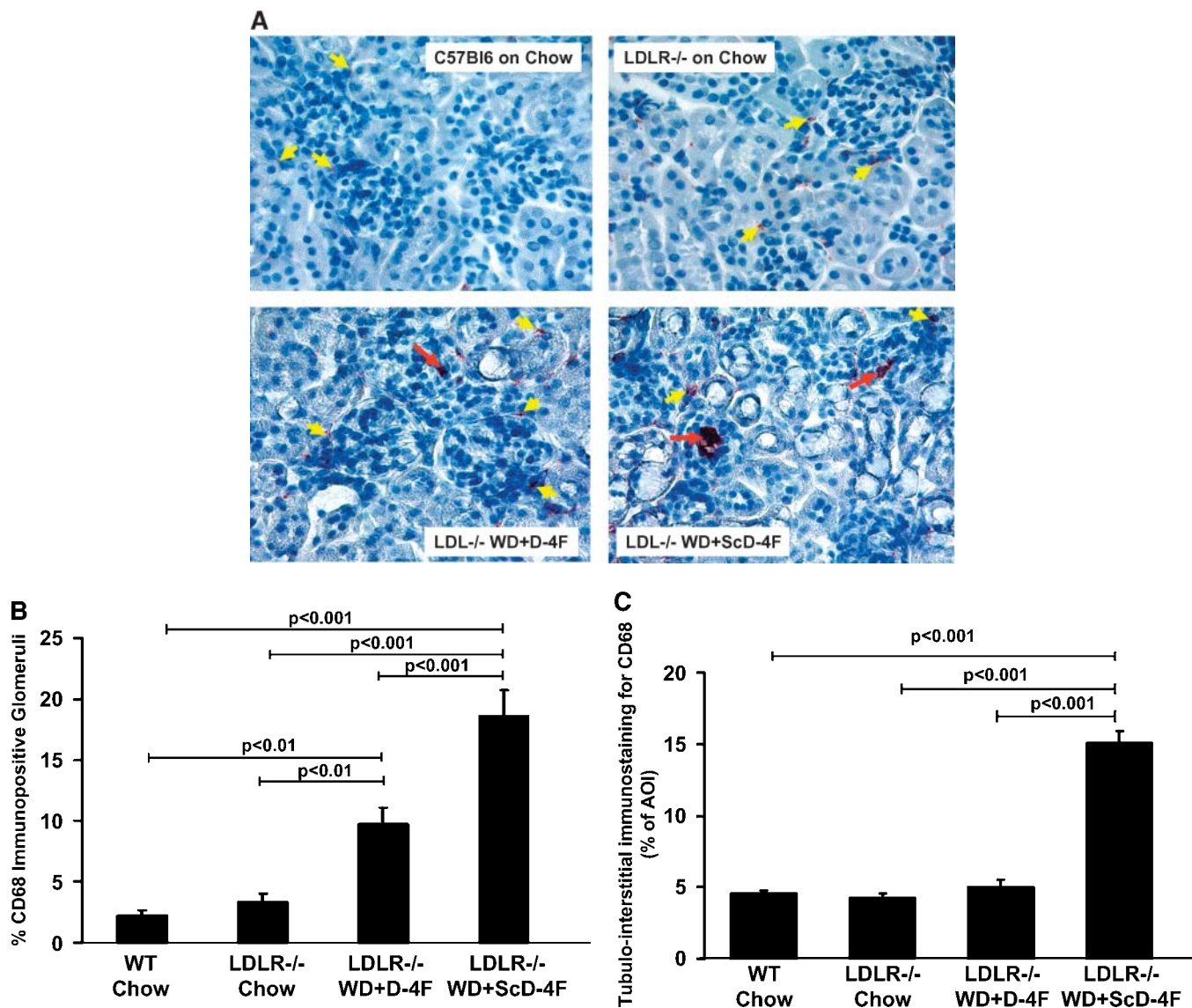


Fig. 7. A: Representative examples of unperfused, frozen kidney sections immunostained for CD68 (brown color) and counterstained with hematoxylin from C57BL/6J mice on chow (upper left panel), LDLR^{-/-} mice on chow (upper right panel), LDLR^{-/-} mice on the WD plus D-4F (lower left panel), and LDLR^{-/-} mice on the WD plus ScD-4F (lower right panel). Few glomeruli contained CD68 macrophages in the chow-fed mice. Red arrows indicate the dark-brown-stained macrophages in the glomeruli of D-4F- and ScD-4F-treated mice. Yellow arrows show the CD68 macrophages in the tubulo-interstitium. Magnification $\times 200$. B: The WD induced an increase in the percent of CD68-immunopositive glomeruli in the kidneys of the LDLR^{-/-} mice compared with the kidneys of LDLR^{-/-} or wild-type C57BL/6J mice (WT) fed a regular chow diet. In the WD plus ScD-4F mice, the percent of CD68-immunopositive glomeruli was significantly higher than in the WD plus D-4F mice. C: The WD induced a significant increase in the percent of the tubulo-interstitial area (expressed as percent AOI) immunostained for CD68 in the kidneys of mice treated with ScD-4F compared with mice treated with D-4F or the chow-fed mice. D: Representative examples of unperfused, frozen kidney sections showing F4/80-immunopositive periglomerular areas (stained in dark-brown color and marked with red arrows) in the kidneys of C67BL/6J mice on chow (upper left panel), LDLR^{-/-} mice on chow (upper right panel), LDLR^{-/-} mice on the WD plus D-4F (lower left panel), and LDLR^{-/-} mice on the WD plus ScD-4F (lower right panel). Note the abundant periglomerular immunostaining in the ScD-4F kidneys compared with the sparse immunostaining present in all the other groups. Magnification $\times 200$. E: The WD induced an increase in the percent of the periglomerular area immunostained for F4/80 macrophages (expressed as percent AOI) in the kidneys. There was a >4 -fold increase in F4/80 immunostaining in the periglomerular area of WD+ScD-4F mice. In contrast, there was only about a 1.6-fold increase in the WD+D-4F mice. Data shown in B, C, and E are mean \pm SEM ($n = 15$ mice per group).

Examination of the capillary contour in the glomerular tuft of the ScD-4F mice showed fewer normal and more dilated capillaries than in the D-4F mice, where there were significantly more normal, clear capillaries ($P < 0.001$) and very few dilated capillaries in the glomerular tuft (Fig. 5).

D-4F decreases WD-induced kidney MCP-1/CCL2

Immunostaining for the chemokine MCP-1/CCL2 showed relatively few immunopositive areas in both the glomerulus (Fig. 6A, B) and in the tubulo-interstitium (Fig. 6C, D) of the D-4F-treated kidneys compared with both the glo-

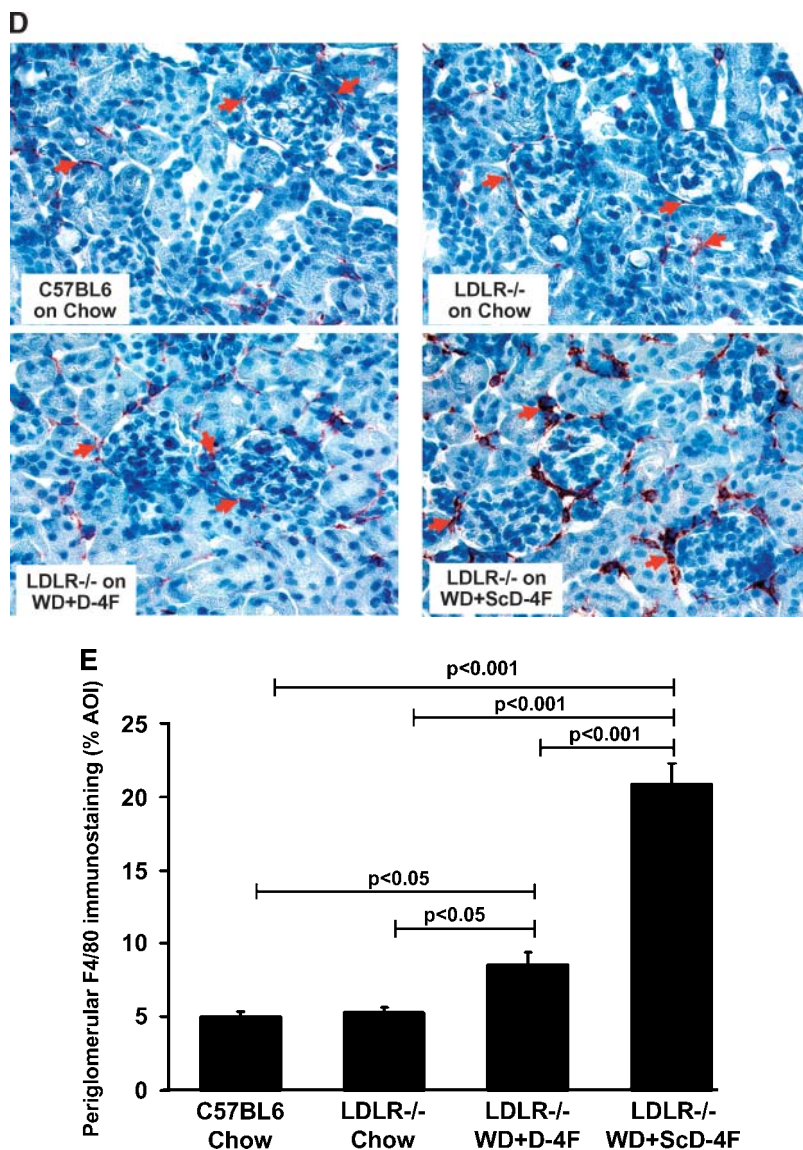


Fig. 7.—Continued.

meruli ($P < 0.0001$) and tubulo-interstitial areas ($P < 0.0183$) of the control ScD-4F kidneys. Owing to the disruption in the visceral membrane of Bowman's capsule, some of the glomerular content spilled into the capsular space of the control ScD-4F mice and immunostained for MCP-1/CCL2 (Fig. 6B). Except for glomeruli showing disruption in the visceral membrane of Bowman's capsule, immunostaining for MCP-1/CCL2 was closely associated with cellular structures in the glomeruli and in the tubulo-interstitial areas.

D-4F reduces WD-induced macrophage accumulation in kidney cortex

Owing to the heterogeneity of macrophage antigen expression in mouse kidney, there have been conflicting reports regarding macrophage distribution in the kidney (30). Therefore, we immunostained for two groups of macrophage antigens, CD68 and F4/80. As Fig. 7 shows, CD68 macrophage immunolabeling was present in both

the tubulo-interstitial areas and in the glomeruli. A very small percent of glomeruli were positive for the CD68 antigen in the chow-fed mice, with a significant increase in the WD-fed mice (Fig. 7A, B). Although the mice on the WD that were treated with D-4F showed a significant increase in the percent of glomeruli immunopositive for the CD68 antigen when compared with the chow-fed LDLR^{-/-} mice, the CD68 values in the D-4F kidneys were significantly lower than those in the control ScD-4F kidneys ($P < 0.001$) (Fig. 7B).

Quantification of tubulo-interstitial CD68 immunostaining revealed a marked accumulation of CD68 macrophages in the kidneys of the control ScD-4F mice, with significantly less immunolabeling in the D-4F-treated mice, with levels of immunostaining in the D-4F-treated mice comparable to those of the chow-fed mice (Fig. 7C).

In contrast to CD68, and confirming the report of Masaki et al. (30), there were no F4/80-labeled macrophages in the glomeruli. F4/80-labeled macrophages were found

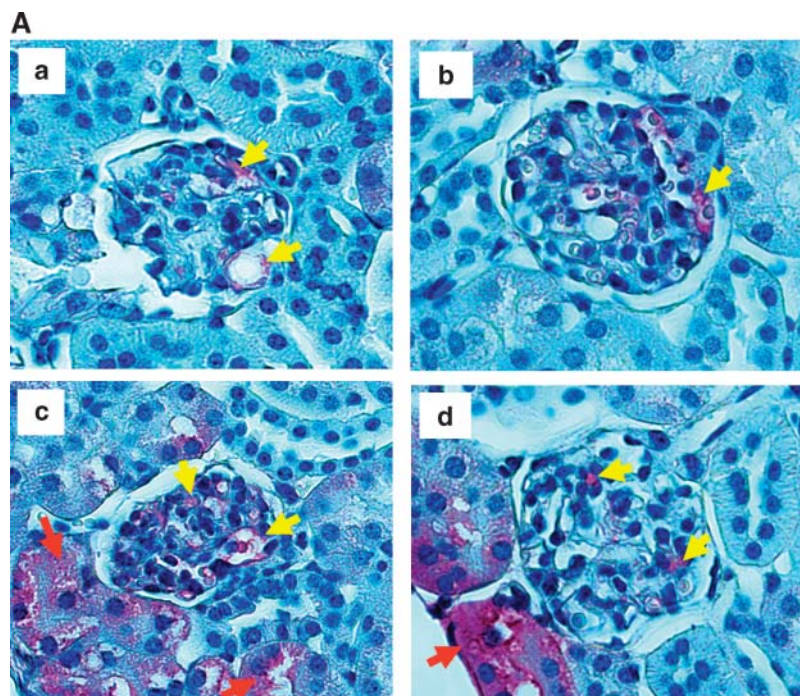


Fig. 8. A: Representative examples of perfused, paraffin-embedded sections of glomeruli and the surrounding tubules immunostained with EO6 antibody in the kidney cortex of LDLR^{-/-} mice on a WD with the control ScD-4F peptide in their drinking water. The sections show glomerular immunostaining in the absence or the presence of tubular immunostaining. Yellow arrows indicate the immunostained cells in the glomerulus and red arrows show the EO6-stained tubular epithelial cells. Panel (a.) shows an EO6-stained capillary wall in the glomerulus. Panel (b.) shows the presence of EO6 immunostaining in the glomerulus with the surrounding tubules unstained. Panel (c.) shows the presence of EO6 immunostaining in the glomerulus with the surrounding tubules moderately immunopositive. Panel (d.) shows the presence of EO6 immunostaining in the glomerulus with the tubules on the left side intensely EO6 immunopositive and negatively stained on the right side. Magnification $\times 400$. B: Representative examples of perfused and paraffin-embedded sections of kidney cortex immunostained with EO6 antibody and counterstained with hematoxylin from C57BL/6J mice on chow (upper left panel), LDLR^{-/-} mice on chow (upper right panel), LDLR^{-/-} mice on WD plus D-4F treatment (lower left panel), and LDLR^{-/-} mice on WD plus control inactive peptide ScD-4F treatment (lower right panel). Oxidized phospholipids recognized by EO6 are stained in red in the glomeruli of the WD plus ScD-4F mice and are indicated by red arrows (lower right panel). Few glomeruli were EO6 immunopositive in the other experimental groups. The yellow arrows indicate EO6-immunopositive tubular epithelium. Magnification $\times 200$. C: Increase in the percent of EO6-immunopositive glomeruli in the kidneys of LDLR^{-/-} mice on the WD treated with ScD-4F compared with mice treated with the active peptide D-4F or the chow-fed mice. D: Increase in the percent of the tubulo-interstitial area (expressed as percent AOI) immunostained for EO6 in the kidneys of LDLR^{-/-} mice treated with the control inactive peptide ScD-4F compared with mice treated with the active peptide D-4F or the chow-fed mice. E: Representative examples of perfused and paraffin-embedded sections of kidney cortex immunostained with LF3 monoclonal antibody against apolipoprotein B (apoB) and counterstained with hematoxylin from C57BL/6J mice on chow (upper left panel), LDLR^{-/-} mice on chow (upper right panel), LDLR^{-/-} mice on WD plus D-4F (lower left panel), and LDLR^{-/-} mice on WD plus ScD-4F (lower right panel). ApoB-immunolabeled structures are stained in red. Magnification $\times 200$. F: Increase in the percent of LF3-immunopositive glomeruli in the kidneys of the LDLR^{-/-} mice on WD treated with the control inactive ScD-4F peptide compared with wild-type mice on chow. No significant differences were found between the other experimental groups. G: Increase in the percent of the tubulo-interstitial area (expressed as percent AOI) immunostained for apoB with the LF3 monoclonal antibody in the kidneys of the LDLR^{-/-} mice on the WD compared with the chow-fed mice. Data shown for C, D, F, G are mean \pm SEM (n = 15 mice per group).

adjacent to Bowman's capsule, in close proximity to and tightly connected with the parietal wall of Bowman's capsule (31) (Fig. 7D). Quantification of the F4/80-immunolabeled periglomerular areas showed that approximately 5% of the area stained positive for F4/80 in the chow-fed mice, with a significant increase in F4/80 immunostaining in mice fed the WD (Fig. 7E). There was a >4-fold increase in F4/80 immunolabeling in the mice fed the WD and treated with the inactive peptide ScD-4F ($P < 0.001$) compared with an approximately 1.6-fold increase in the mice on the WD that received D-4F ($P < 0.001$) (Fig. 7E). The combined CD68 and F4/80 data strongly suggest

that the WD induced an inflammatory process characterized by increased macrophage presence in the kidneys, which was largely ameliorated by D-4F treatment but not by treatment with ScD-4F.

D-4F reduces WD-induced renal oxidized phospholipids without altering apoB

The presence of oxidized phospholipid epitopes recognized by the monoclonal antibody EO6 was demonstrated in both the glomeruli and in tubulo-interstitial areas (Fig. 8). Less than 5% of glomeruli of C57BL/6J mice on chow were EO6 immunopositive. In contrast, ap-

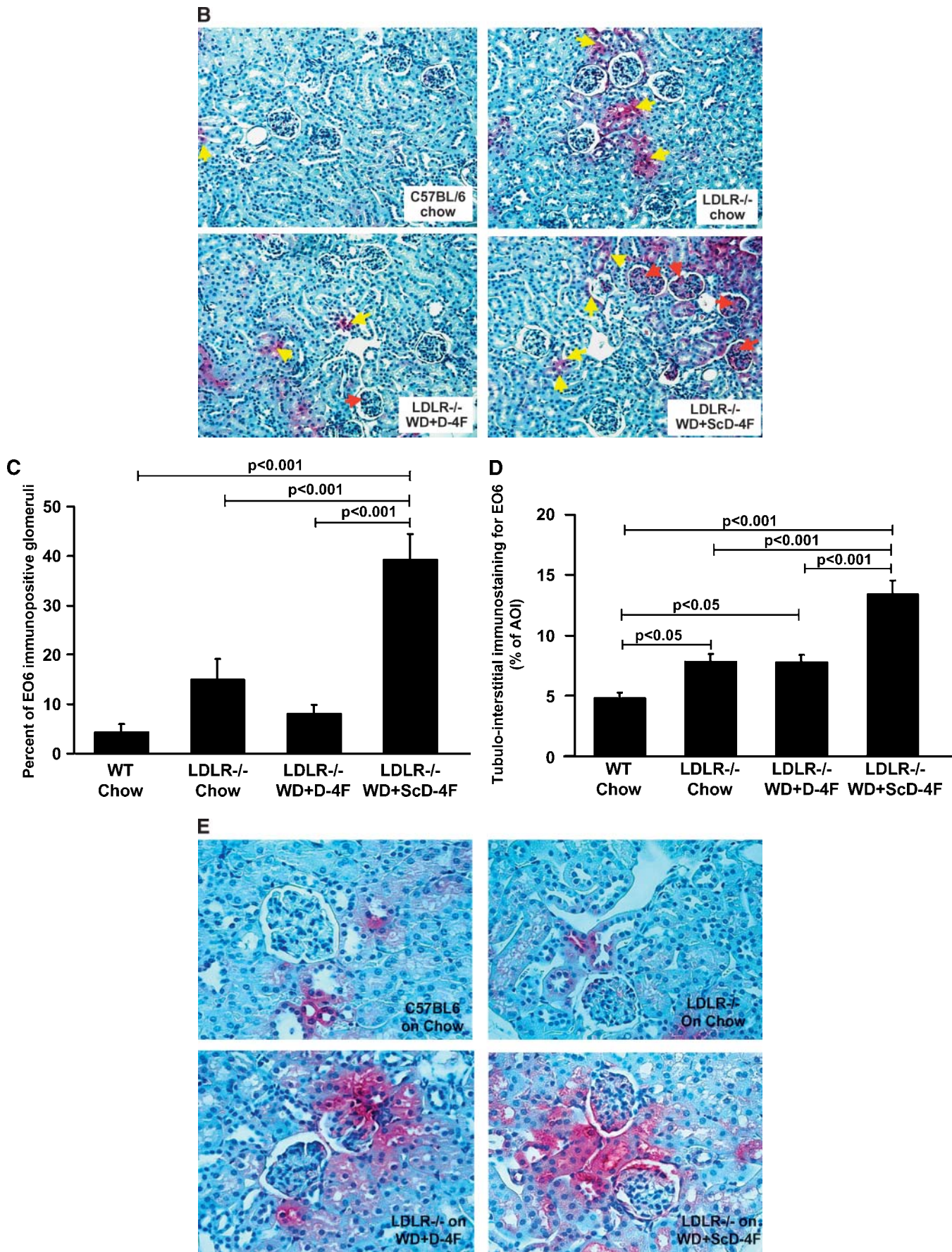


Fig. 8.—Continued.

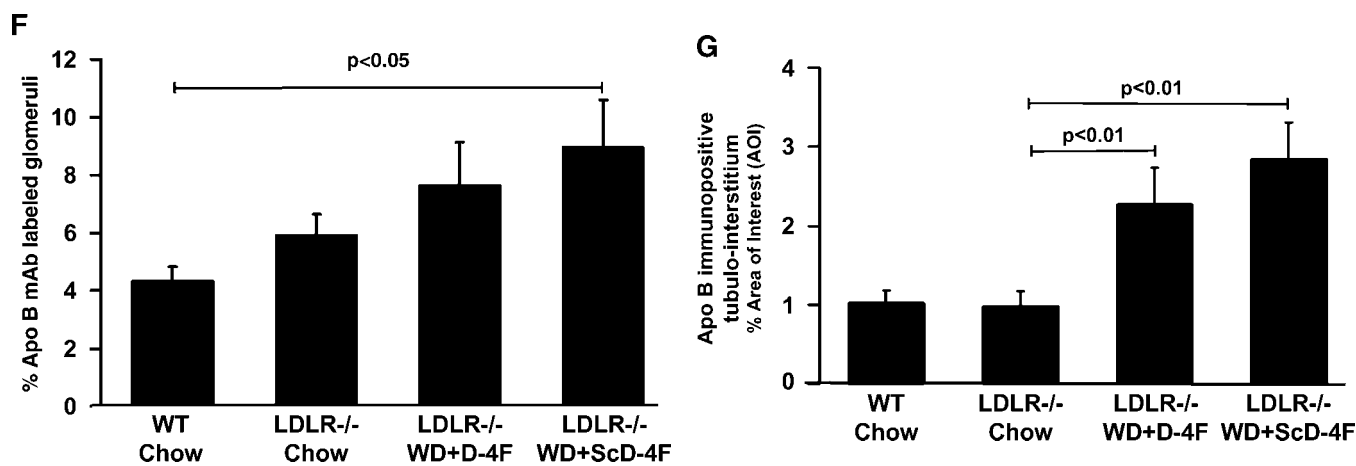


Fig. 8.—Continued.

proximately 40% of the glomeruli in $LDLR^{-/-}$ mice on WD treated with the control inactive peptide ScD-4F were EO6 immunopositive, and there was a highly significant difference between these mice and the other three groups. The differences between C57BL/6J mice on chow, $LDLR^{-/-}$ mice on chow, and $LDLR^{-/-}$ mice on the WD with D-4F treatment were not significant (Fig. 8C). EO6 immunostaining of the tubulo-interstitial areas revealed a significant increase in the $LDLR^{-/-}$ mice on chow compared with the wild-type C57BL/6J mice on chow. EO6 immunostaining of the tubulo-interstitial areas of $LDLR^{-/-}$ mice on the WD treated with the inactive control ScD-4F peptide was significantly higher than in $LDLR^{-/-}$ mice on chow or $LDLR^{-/-}$ mice on the WD with D-4F treatment. There was no significant difference in EO6 immunostaining of the tubulo-interstitial areas of $LDLR^{-/-}$ mice on chow compared with $LDLR^{-/-}$ mice on the WD with D-4F treatment (Fig. 8D).

Although there was a highly significant increase in EO6 immunostaining in the kidneys of $LDLR^{-/-}$ mice on the WD treated with the inactive control ScD-4F peptide compared with $LDLR^{-/-}$ mice on the WD treated with D-4F (Fig. 8B–D), there was no significant difference in apoB immunostaining of the glomeruli or the tubulo-interstitial areas (Fig. 8E–G). There was a significant increase in apoB immunostaining between the mice on the WD compared with the mice on the chow diet, but there was no significant difference in apoB immunostaining in mice on the WD treated with the inactive control ScD-4F peptide compared with those treated with the active D-4F peptide (Fig. 8E–G). Similarly, there was a highly significant difference in plasma lipid and lipoprotein levels between chow-fed mice and mice fed the WD, but there was no significant difference in plasma lipid and lipoprotein levels in mice fed the WD and treated with ScD-4F compared with those treated with D-4F (Table 1).

D-4F treatment prevents the dramatic increase in SREBP-1c mRNA levels induced by feeding $LDLR^{-/-}$ mice a WD

On the basis of the work of Jiang and colleagues (7) and Berliner and colleagues (10, 11), we hypothesized that the

WD would increase SREBP-1c mRNA levels and kidney triglyceride levels. We further hypothesized that these changes would be ameliorated by D-4F treatment. Using quantitative PCR, we found that kidney SREBP-1c mRNA levels were low in C57BL/6J wild-type mice on a chow diet. There was a trend toward higher levels in $LDLR^{-/-}$ mice on chow, but this increase did not reach statistical significance (Fig. 9). As predicted by the work of Jiang et al. (7), there was a dramatic increase in kidney SREBP-1c mRNA levels in the mice fed the WD and treated with the control inactive ScD-4F peptide. Berliner and colleagues (10, 11) demonstrated that oxidized phospholipids induce SREBP. Mice fed the WD and treated with the active peptide D-4F had renal levels of oxidized phospholipids not significantly different from $LDLR^{-/-}$ mice on chow (Fig. 8). The mice fed the WD and treated with D-4F also had kidney levels of SREBP-1c mRNA that were not significantly different from $LDLR^{-/-}$ mice on chow (Fig. 9). Consistent with the increased SREBP-1c mRNA levels in the control mice on the WD, kidney triglyceride levels were significantly increased in the mice on the WD that were treated with the control inactive ScD-4F peptide but were not increased in mice on the WD that were treated with the active D-4F peptide (Table 1). As shown in Table 1, there was a significant increase in kidney weight in mice on the WD, but there was no significant difference in kidney weight between mice treated with the control inactive ScD-4F peptide and those treated with the active D-4F peptide. Kidney total cholesterol levels in mice on a WD treated with the control inactive ScD-4F peptide were significantly higher compared with those of C57BL/6J wild-type mice on chow, but there was no significant difference compared with $LDLR^{-/-}$ mice on chow or on the WD with D-4F treatment. (Table 1).

DISCUSSION

After feeding C57BL/6J mice a 60 kcal% saturated (lard) fat diet for 12 weeks, Jiang et al. (7) observed a significant increase in kidney triglyceride levels with a

TABLE 1. Measurements of body weight, systolic blood pressure, plasma lipids and lipoproteins, glucose, blood urea nitrogen, urine albumin, kidney weight, kidney total cholesterol content, and kidney triglyceride content

Parameters	I. C57BL/6 on Chow	II. LDLR ^{-/-} on Chow	III. LDLR ^{-/-} on WD + D-4F	IV. LDLR ^{-/-} on WD + Sc D-4F
Body weight (g)	18.3 ± 0.2	18.6 ± 0.3	22.1 ± 0.5 ^{b***}	24.6 ± 0.8 ^{c***}
Systolic BP (mmHg)	101.2 ± 3.1	97.5 ± 1.9	98.9 ± 2.7	102.3 ± 1.5
TC (mg/dl)	173.9 ± 9.3	431.5 ± 16.1 ^{a***}	1435.3 ± 42.5 ^{b***}	1443.5 ± 54.7 ^{c***}
HDL-C (mg/dl)	65.2 ± 3.5	78.4 ± 2.6 ^{b***}	74.8 ± 3.5 ^{f***}	76.4 ± 3.8 ^{f***}
HDL-C/TC ratio	0.375 ± 0.02	0.181 ± 0.006 ^{f***}	0.052 ± 0.002 ^{f***,d***}	0.053 ± 0.002 ^{f***,c***}
TG (mg/dl)	90.4 ± 12.2	146.4 ± 23.1	319.2 ± 33.9 ^{b***,d*}	388.2 ± 51.8 ^{c***}
LDL-C + VLDL-C (mg/dl)	90.6 ± 8.7	324.8 ± 14.2 ^{a***}	1296.6 ± 31.3 ^{b,d***}	1289.4 ± 77.4 ^{c,c***}
Glucose (mg/dl)	203.6 ± 7.9	227.1 ± 10.4	293.5 ± 8.4 ^{b,d***}	304.9 ± 14.6 ^{c,c***}
BUN (mg/dl)	—	15.0 ± 0.7	14.9 ± 0.8	14.8 ± 1.0
Urine albumin (mg/dl)	—	0.0265 ± 0.001	0.0256 ± 0.001	0.0262 ± 0.002
Kidney weight (g)	0.0989 ± 0.0037	0.0937 ± 0.0029	0.1118 ± 0.0027 ^{b*,d***}	0.1078 ± 0.002 ^{c***}
Kidney TC (μg/mg wet weight)	10.441 ± 1.157	13.403 ± 1.648	14.406 ± 1.102	17.001 ± 1.800 [*]
Kidney TG (μg/mg wet weight)	15.369 ± 3.467	16.541 ± 1.984	19.957 ± 3.169	32.910 ± 3.409 ^{c***,c***,g*}

BP, blood pressure; BUN, blood urea nitrogen; HDL-C, HDL-cholesterol; LDL-C, LDL-cholesterol; TC, total cholesterol; TG, triglyceride; VLDL-C, very low density cholesterol; WD, Western diet. Data are expressed as mean ± SEM.

- ^a I versus II.
- ^b I versus III.
- ^c I versus IV.
- ^d II versus III.
- ^e II versus IV.
- ^f I versus II, III, IV.
- ^g III versus IV.
- * $P < 0.05$.
- ** $P < 0.01$.
- *** $P < 0.001$.

trend toward increased kidney cholesterol levels that was not statistically significant. These changes were associated with a significant increase in the expression of SREBP and significant increases in mRNA levels for genes known to be regulated by SREBP-1c (e.g., acetyl-CoA carboxylase and fatty acid synthase) as well as significant increases in mRNA levels for genes implicated in glomerulosclerosis [e.g., plasminogen activator inhibitor-1 (PAI-1), vascular endothelial growth factor (VEGF), type IV collagen, and

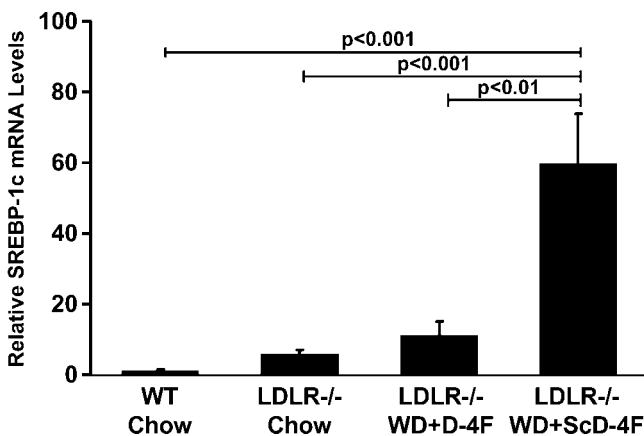



Fig. 9. D-4F treatment prevents the dramatic increase in sterol-regulatory element binding protein-1c (SREBP-1c) mRNA levels induced by feeding LDLR^{-/-} mice a WD. SREBP-1c mRNA levels were determined by quantitative PCR analysis as described in Materials and Methods in C57BL/6J WT mice on chow, in LDLR^{-/-} mice on chow, and in LDLR^{-/-} mice on the WD treated with the active peptide (WD+D-4F) or the inactive control ScD-4F peptide (WD+ScD-4F). Data are expressed as mean ± SEM (n = 4 mice per group). The results are representative of two out of two separate experiments.

fibronectin]. These mice also demonstrated increased PAS staining, which is a hallmark of mesangial expansion. In mice lacking SREBP-1c, the diet failed to induce an increase in renal triglyceride levels, and the induction of PAI-1, VEGF, type IV collagen, and fibronectin was markedly attenuated. The authors concluded that diet-induced obesity in the C57BL/6J mice caused increased renal lipid accumulation and glomerulosclerosis via an SREBP-1c-dependent pathway (7).

The plasma lipid changes in the wild-type C57BL/6J mice on the high-fat diet in the studies of Jiang et al. (7) were much less than was the case in our studies with LDLR^{-/-} mice on a WD. Plasma total cholesterol levels were 223 ± 16 mg/dl in Jiang's study compared with 1,444 ± 55 mg/dl in LDLR^{-/-} mice on the WD and treated with ScD-4F (Table 1). Similarly, plasma triglycerides in Jiang's study were 105 ± 7 mg/dl versus 388 ± 52 mg/dl in LDLR^{-/-} mice on WD and treated with ScD-4F (Table 1). Plasma glucose levels were also different but less so, with values of 216 ± 16 mg/dl in Jiang's study compared with values of 305 ± 15 mg/dl in LDLR^{-/-} mice on the WD and treated with ScD-4F (Table 1). Interestingly, Jiang and colleagues (7) found proteinuria and we did not. This may have been due to the fact that the mice in Jiang's study were slightly older at the start of the study (8 versus 7 weeks) and were maintained on the high-fat diet for almost twice as long as was the case in our study (12 versus 7 weeks). Additionally, the composition of the WD is significantly different compared with the diet in Jiang's study, and we studied the effects of the WD in LDLR^{-/-} mice on a C57BL/6J background, whereas Jiang and colleagues studied wild-type C57BL/6J mice (7).

Similar to the findings of Jiang et al. (7), on feeding LDLR^{-/-} mice the WD, we found that they developed

glomerular changes, including evidence of mesangial expansion (Figs. 1–5). Additionally, we found evidence of chronic inflammation, such as increased expression of the potent monocyte chemoattractant MCP-1 (Fig. 6), and evidence of increased renal macrophage content (Fig. 7). The increase in MCP-1 and in macrophages in the kidney is similar to the inflammatory changes that were previously seen in the aorta (1) and in the brain (3) after feeding a WD to LDLR^{-/-} mice. These inflammatory changes are precisely what would be expected from an accumulation of oxidized phospholipids (9). Indeed, we found a marked increase in renal oxidized phospholipids (Fig. 8A–E). We also found a significant increase in renal triglycerides (Table 1), and renal SREBP-1c mRNA levels (Fig. 9). In contrast to these changes in the LDLR^{-/-} mice on the WD treated with the control inactive ScD-4F peptide, treating the mice with the active D-4F peptide resulted in a significant reduction in renal oxidized phospholipids (Fig. 8A–E), triglycerides (Table 1), and renal SREBP-1c mRNA levels (Fig. 9). The reduction in renal oxidized phospholipids, renal triglyceride levels, and renal SREBP-1c mRNA levels in the D-4F-treated mice occurred without a change in plasma lipid, lipoprotein, or glucose levels, without a change in renal apoB levels, and without a change in blood pressure (Table 1). Moreover, the reduction in renal oxidized phospholipids, renal triglyceride levels, and renal SREBP-1c mRNA levels with D-4F treatment was accompanied by a significant reduction in mesangial expansion and other glomerular changes (Figs. 1–5), and a significant reduction in renal MCP-1 (Fig. 6) and renal macrophage content (Fig. 7).

Yeh et al. (10) reported that oxidized phospholipids that are recognized by EO6 (16–18) dramatically induced the expression of SREBP, which was required for the oxidized phospholipids to induce cytokine expression in endothelial cells. We think the most likely explanation for the findings reported here is that the apoA-I mimetic peptide D-4F reduced the tissue levels of oxidized phospholipids, resulting in significantly less SREBP-1c expression, less renal triglyceride accumulation, less cytokine production, and less inflammation without changing plasma lipid, lipoprotein, or glucose levels, without a change in renal apoB levels, and without a change in blood pressure. This scenario is consistent with the proposed mechanism of action for apoA-I mimetic peptides, in which they provide a thermodynamically stable environment for binding, sequestering, and removing pro-inflammatory oxidized lipids (32). 

This work was supported in part by US Public Health Service grants HL-30568 and HL-34343 and the Laubisch, Castera, and M. K. Grey Funds at the University of California, Los Angeles.

REFERENCES

- Navab, M., G. M. Anantharamaiah, S. Hama, D. W. Garber, M. Chaddha, G. Hough, R. Lallone, and A. M. Fogelman. 2002. Oral administration of an apo A-I mimetic peptide synthesized from D-amino acids dramatically reduces atherosclerosis in mice independent of plasma cholesterol. *Circulation*. **105**: 290–292.
- Ou, J., J. Wang, H. Xu, Z. Ou, M. G. Sorci-Thomas, D. W. Jones, P. Signorino, J. C. Densmore, S. Kaul, K. T. Oldham, et al. 2005. Effects of D-4F on vasodilation and vessel wall thickness in hypercholesterolemic LDL receptor-null and LDL receptor/apolipoprotein A-I double-knockout mice on Western diet. *Circ. Res.* **97**: 1190–1197.
- Buga, G. M., J. S. Frank, G. A. Mottino, M. Hendizadeh, A. Hakhamian, J. H. Tillisch, S. T. Reddy, M. Navab, G. M. Anantharamaiah, L. J. Ignarro, et al. 2006. D-4F decreases brain arteriole inflammation and improves cognitive performance in LDL receptor-null mice on a Western diet. *J. Lipid Res.* **47**: 2148–2160.
- Merat, S., F. Casanada, M. Sutphin, W. Palinski, and P. D. Reaven. 1999. Western-type diets induce insulin resistance and hyperinsulinemia in LDL receptor-deficient mice but do not increase aortic atherosclerosis compared with normoinsulinemic mice in which similar plasma cholesterol levels are achieved by a fructose-rich diet. *Arterioscler. Thromb. Vasc. Biol.* **19**: 1223–1230.
- Schreyer, S. A., C. Vick, T. C. Lystig, P. Mystkowski, and R. C. LeBoeuf. 2002. LDL receptor but not apolipoprotein E deficiency increases diet-induced obesity and diabetes in mice. *Am. J. Physiol. Endocrinol. Metab.* **282**: e207–e214.
- Keane, W. F., and P. A. Lyle. 2005. Kidney disease and cardiovascular disease: implications of dyslipidemia. *Cardiol. Clin.* **23**: 363–372.
- Jiang, T., Z. Wang, G. Proctor, S. Moskowitz, S. E. Liebman, T. Rogers, M. S. Lucia, J. Li, and M. Levi. 2005. Diet-induced obesity in C57BL/6J mice causes increased renal lipid accumulation and glomerulosclerosis via a sterol regulatory element-binding protein-1c-dependent pathway. *J. Biol. Chem.* **280**: 32317–32325.
- Fogelman, A. M. 2005. When pouring water on the fire makes it burn brighter. *Cell Metab.* **2**: 6–8.
- Berliner, J. A., and A. D. Watson. 2005. A role for oxidized phospholipids in atherosclerosis. *N. Engl. J. Med.* **353**: 9–11.
- Yeh, M., A. L. Cole, J. Choi, Y. Liu, D. Tulchinsky, J. H. Qiao, M. C. Fishbein, A. N. Dooley, T. Hovnanian, K. Mouilleteaux, et al. 2004. Role for sterol regulatory element-binding protein in activation of endothelial cells by phospholipid oxidation products. *Circ. Res.* **95**: 780–788.
- Gharavi, N. M., N. A. Baker, K. P. Mouilleteaux, W. Yeung, H. M. Honda, X. Hsieh, M. Yeh, E. J. Smart, and J. A. Berliner. 2006. Role of endothelial nitric oxide synthase in the regulation of SREBP activation by oxidized phospholipids. *Circ. Res.* **98**: 768–776.
- Ou, Z., J. Ou, A. W. Ackerman, K. T. Oldham, and K. A. Pritchard, Jr. 2003. L-4F, an apolipoprotein A-I mimetic, restores nitric oxide and superoxide anion balance in low-density lipoprotein-treated endothelial cells. *Circulation*. **107**: 1520–1524.
- Ou, J., Z. Ou, D. W. Jones, S. Holzhauser, O. A. Hatoum, A. W. Ackerman, D. W. Weihrauch, D. D. Gutterman, K. Guice, K. T. Oldham, et al. 2003. L-4F, an apolipoprotein mimetic, dramatically improves vasodilation in hypercholesterolemia and sickle cell disease. *Circulation*. **107**: 2337–2341.
- Weihrauch, D., H. Xu, Y. Shi, J. Wang, J. Brien, D. W. Jones, S. Kaul, R. A. Komorowski, M. E. Csuka, K. T. Oldham, et al. 2007. Effects of D-4F on vasodilation, oxidative stress, angiostatin, myocardial inflammation, and angiogenic potential in tight-skin mice. *Am. J. Physiol. Heart Circ. Physiol.* **293**: H1432–H1441.
- Van Lenten, B. J., A. C. Wagner, M. Navab, G. M. Anantharamaiah, E. K. Hui, D. P. Nayak, and A. M. Fogelman. 2004. D-4F, an apolipoprotein A-I mimetic peptide, inhibits the inflammatory response induced by influenza A infection of human type II pneumocytes. *Circulation*. **110**: 3252–3258.
- Palinski, W., S. Horkko, E. Miller, U. P. Steinbrecher, H. C. Powell, L. K. Curtiss, and J. L. Witztum. 1996. Cloning of monoclonal autoantibodies to epitopes of oxidized lipoproteins from apolipoprotein E-deficient mice. Demonstration of epitopes of oxidized low density lipoprotein in human plasma. *J. Clin. Invest.* **98**: 800–814.
- Watson, A. D., N. Leitinger, M. Navab, K. F. Faull, S. Horkko, J. L. Witztum, W. Palinski, D. Schwenke, R. G. Salomon, W. Sha, et al. 1997. Structural identification by mass spectrometry of oxidized phospholipids in minimally oxidized low density lipoprotein that induce monocyte/endothelial interactions and evidence for their presence in vivo. *J. Biol. Chem.* **272**: 13597–13607.
- Horkko, S., D. A. Bird, E. Miller, H. Itabe, N. Leitinger, G. Subbanagounder, J. A. Berliner, P. Friedman, E. A. Dennis, L. K. Curtiss, et al. 1999. Monoclonal autoantibodies specific for oxidized phospholipids or oxidized phospholipid-protein adducts in-

- hibit macrophage uptake of oxidized low-density lipoproteins. *J. Clin. Invest.* **103**: 117–128.
19. Zlot, C. H., L. M. Flynn, M. M. Veniant, E. Kim, M. Raabe, S. P. McCormick, P. Ambroziak, L. M. McEvoy, and S. G. Young. 1999. Generation of monoclonal antibodies specific for mouse apolipoprotein B-100 in apolipoprotein B-48-only mice. *J. Lipid Res.* **40**: 76–84.
 20. Feng, X., H. Li, A. A. Rumbin, X. Wang, A. La Cava, K. Brechtelsbauer, L. W. Castellani, J. L. Witztum, A. J. Lusis, and B. P. Tsao. 2007. ApoE^{-/-}Fas^{-/-} C57BL/6 mice: a novel murine model simultaneously exhibits lupus nephritis, atherosclerosis, and osteopenia. *J. Lipid Res.* **48**: 794–805.
 21. Zoja, C., D. Corna, D. Rottoli, C. Zanchi, M. Abbate, and G. Remuzzi. 2006. Imatinib ameliorates renal disease and survival in murine lupus autoimmune disease. *Kidney Int.* **70**: 97–103.
 22. Spencer, M. W., A. S. Muhlfeld, S. Segerer, K. L. Hudkins, E. Kirk, R. C. LeBoeuf, and C. E. Alpers. 2004. Hyperglycemia and hyperlipidemia act synergistically to induce renal disease in LDL receptor-deficient BALB mice. *Am. J. Nephrol.* **24**: 20–31.
 23. Muhlfeld, A. S., M. W. Spencer, K. L. Hudkins, E. Kirk, R. C. LeBoeuf, and C. E. Alpers. 2004. Hyperlipidemia aggravates renal disease in B6.ROP Os/+ mice. *Kidney Int.* **66**: 1393–1402.
 24. Wen, M., S. Segerer, M. Dantas, P. A. Brown, K. L. Hudkins, T. Goodpaster, E. Kirk, R. C. LeBoeuf, and C. E. Alpers. 2002. Renal injury in apolipoprotein E-deficient mice. *Lab. Invest.* **82**: 999–1006.
 25. Yang, J., J. L. Goldstein, R. E. Hammer, Y. A. Moon, M. S. Brown, and J. D. Horton. 2001. Decreased lipid synthesis in livers of mice with disrupted Site-1 protease gene. *Proc. Natl. Acad. Sci. USA.* **98**: 13607–13612.
 26. Navab, M., S. Y. Hama, C. J. Cooke, G. M. Anantharamaiah, M. Chaddha, L. Jin, G. Subbanagounder, K. F. Faull, S. T. Reddy, N. E. Miller, et al. 2000. Normal high density lipoprotein inhibits three steps in the formation of mildly oxidized low density lipoprotein: step 1. *J. Lipid Res.* **41**: 1481–1494.
 27. Kamanna, V. S., R. Pai, D. D. Roh, and M. A. Kirschenbaum. 1996. Oxidative modification of low-density lipoprotein enhances the murine mesangial cell cytokines associated with monocyte migration, differentiation, and proliferation. *Lab. Invest.* **74**: 1067–1079.
 28. Kamanna, V. S., R. Pai, H. Ha, M. A. Kirschenbaum, and D. D. Roh. 1999. Oxidized low-density lipoprotein stimulates monocyte adhesion to glomerular endothelial cells. *Kidney Int.* **55**: 2192–2202.
 29. Pai, R., H. Ha, M. A. Kirschenbaum, and V. S. Kamanna. 1996. Role of tumor necrosis factor-alpha on mesangial cell MCP-1 expression and monocyte migration: mechanisms mediated by signal transduction. *J. Am. Soc. Nephrol.* **7**: 914–923.
 30. Masaki, T., F. Chow, D. J. Nikolic-Paterson, R. C. Atkins, and G. H. Tesch. 2003. Heterogeneity of antigen expression explains controversy over glomerular macrophage accumulation in mouse glomerulonephritis. *Nephrol. Dial. Transplant.* **18**: 178–181.
 31. Hume, D. A., and S. Gordon. 1983. Mononuclear phagocyte system of the mouse defined by immunohistochemical localization of antigen F4/80. Identification of resident macrophages in renal medullary and cortical interstitium and the juxtaglomerular complex. *J. Exp. Med.* **157**: 1704–1709.
 32. Anantharamaiah, G. M., V. K. Mishra, D. W. Garber, G. Datta, S. P. Handattu, M. N. Palgunachari, M. Chaddha, M. Navab, S. T. Reddy, J. P. Segrest, et al. 2007. Structural requirements for anti-oxidative and anti-inflammatory properties of apolipoprotein A-I mimetic peptides. *J. Lipid Res.* **48**: 1915–1923.